1521-0103/346/1/67–74$25.00
THE JOURNAL OF PHARMACOLOGY AND EXPERIMENTAL THERAPEUTICS

http://dx.doi.org/10.1124/jpet.113.203844
J Pharmacol Exp Ther 346:67–74, July 2013

20-Hydroxyeicosatetraenoic Acid Inhibition Attenuates Balloon Injury-Induced Neointima Formation and Vascular Remodeling in Rat Carotid Arteries

Ludwig D. Orozco, Huiling Liu, Eddie Perkins, Daryl A. Johnson, Betty B. Chen, Fan Fan, Rodney C. Baker, and Richard J. Roman

Department of Neurosurgery (L.D.O., H.L., E.P., D.A.J., B.B.C.), Department of Anatomy (E.P.), and Department of Pharmacology and Toxicology (F.F., R.C.B., R.J.R.), University of Mississippi Medical Center, University of Mississippi, Jackson, Mississippi

Received February 3, 2013; accepted May 7, 2013

ABSTRACT

20-Hydroxyeicosatetraenoic acid (20-HETE) contributes to the migration and proliferation of vascular smooth muscle cells (VSMC) in vitro, but there are few studies that address its effects on vascular remodeling in vivo. The present study determined whether inhibition of 20-HETE production attenuates intimal hyperplasia (IH) and vascular remodeling after balloon injury (BI). Sprague Dawley rats underwent BI of the common carotid artery and were treated with vehicle, 1-aminobenzotriazole (ABT, 50 mg/kg i.p. once daily), or HET0016 (*N*-hydroxy-*N′*-(4-butyl-2-methylphenyl)-formamidine) (2 mg/kg s.c. twice daily) for 14 days. Fourteen days after BI and treatment, the animals underwent carotid angiography, and the arteries were harvested for morphometric, enzymatic and immunohistochemical analysis. There was a 96% reduction of angiographic stenosis in the rats treated with 1-ABT. There was a 61 and 66% reduction of the intima/media area ratios in the 1-ABT and HET0016 treated rats compared with the vehicle-treated group. 20-HETE levels were elevated in BI carotid arteries, and the levels were markedly suppressed in the groups treated with 1-ABT and HET0016 ($P < 0.001$). Immunostaining revealed that the expression of CYP4A enzyme was markedly increased in the neointima of BI arteries, and it colocalized with the expression of smooth muscle-specific actin, indicating increased proliferation of VSMC. An increase in the expression of CYP4A and the production of 20-HETE contributes to neointimal growth in BI rat carotid arteries. Systemic administration 1-ABT or HET0016 prevents the increase in 20-HETE levels and attenuates VSMC migration and proliferation, resulting in a marked reduction in IH and vascular remodeling after endothelial injury.

Introduction

Vascular restenosis due to intimal hyperplasia (IH) remains the major obstacle to satisfactory long-term patency of open and catheter-based treatment of obstructive arterial disease (Wu et al., 2011). Monocytes, macrophages, inflammation, and vascular smooth muscle cell (VSMC) proliferation and migration are thought to be central to the development of IH (Davies and Hagen, 1994; Pietersma et al., 1995; Fujita et al., 1999; Stec et al., 2007; Afergan et al., 2010). Arachidonic acid (AA) is metabolized into prostanoids, leukotrienes, and eicosanoids. Important eicosanoids include epoxyeicosatrienoic acids (EETs) and hydroxyeicosatetraenoic acids (HETEs) such as 5-, 8-, 11-, 12-, 16-, 18-, 19-, and 20-HETE (McGiff, 1981; Capdevila and Falck, 2002; Roman, 2002). Of these, 20-HETE has been shown to play an important role in the regulation of vascular and renal functions (Samuelsson, 1983; Roman, 2002; Liang et al., 2008). 20-HETE is a potent vasoconstrictor that contributes to the development of cerebral vasospasm and ischemia reperfusion injury (Roman, 2002). It has also been reported to stimulate the migration and proliferation of VSMC induced by angiotensin II, vascular endothelial growth factor (VEGF), and platelet-derived growth factor (PDGF) in vitro, but its role in IH after endothelial injury in vivo is less clear (Stern et al., 1989; Lin et al., 1995; Bruijns et al., 1998; Muthalif et al., 1998; Uddin et al., 1998; Patricia et al., 1999; Reddy et al., 2002; Yaghini et al., 2005; Guo et al., 2007; Stec et al., 2007).

There is one report that angiotensin II and AA increase the expression of CYP4A1 in balloon-injured (BI) rat carotid arteries and neointima formation (Yaghini et al., 2005). Administration of a CYP4A1 antisense oligonucleotide attenuated the stimulatory effects of angiotensin II and AA on IH, but it had no effect on neointimal formation under baseline conditions (Yaghini et al., 2005). In the present study, we examined the effects of chronic inhibition of the synthesis of

This work was supported in part by the National Institutes of Health National Heart, Lung, and Blood Institute [Grants HL36279, HL29587] (to R.J.R.).
dx.doi.org/10.1124/jpet.113.203844.

ABBREVIATIONS: AA, arachidonic acid; 1-ABT, 1-aminobenzotriazole; AP, anteroposterior; BI, balloon injury; BSA, bovine serum albumin; EET, epoxyeicosatrienoic acid; HET0016, *N*-hydroxy-*N′*-(4-butyl-2-methylphenyl)-formamidine; HETE, hydroxyeicosatetraenoic acid; IH, intimal hyperplasia; MAPK, mitogen-activated protein kinase; NO, nitric oxide; TBST, Tris-buffered saline/Tween 20; VEGF, vascular endothelial growth factor; VSMC, vascular smooth muscle cells.

20-HETE with 1-aminobenzotriazole (1-ABT) or *N*-hydroxy-*N*′-(4-butyl-2-methyl-phenyl)-formamidine (HET0016) on intimal hyperplasia and vascular remodeling after BI in rat carotid arteries.

Materials and Methods

Experiments were performed in 12-week-old male Sprague-Dawley rats ($N = 30$) obtained from Harlan Laboratories (Indianapolis, IN). The animals had free access to rat chow (Harlan laboratories) and tap water under standard care. All protocols were approved by the Institutional Animal Care and Use Committee at the University of Mississippi Medical Center and were consistent with the U.S. National Institutes of Health *Guide for the Care and Use of Laboratory Animals*.

1-ABT and HET0016 were obtained from Sigma-Aldrich (St. Louis, MO); both drugs were dissolved in 11% sulfobutyl ether β-cyclodextrin (Captisol)/3% mannitol solution. The rats were assigned to three treatment groups. Group 1 was treated with vehicle ($n = 10$), group 2 was treated with 1-ABT ($n = 10$) (50 mg/kg i.p. once per day), and group 3 received HET0016 ($n = 10$) (2 mg /kg s.c. twice daily) (Miyata et al., 2001; Sato et al., 2001; Balani et al., 2002; Xu et al., 2004; Chen et al., 2005; Miyata and Roman, 2005) for a total of 16 days, starting 2 days before BI and continuing until sacrifice on day 14.

Rat Carotid Artery Balloon Injury. This study employed the well-characterized rat carotid artery BI technique (Tulis, 2007). In brief, rats were anesthetized with isoflurane (Kissin et al., 1983), and the left common and external carotid arteries were exposed. A Fogarty 2F arterial embolectomy catheter (Edwards Lifesciences, Irvine, CA) was introduced into the external carotid artery and was advanced 20 mm above the aortic arch. The balloon was inflated to achieve adequate resistance (between 1.8 and 2.2 atm) and then was withdrawn with rotation toward the carotid bifurcation. This was repeated three times. When the catheter was withdrawn, the external carotid was ligated. Immediately after injury, carotid artery pulsatility and patency were checked, and the degree of balloon inflation was validated.

Microangiography of Injured Carotid Arteries. Fourteen days after balloon injury, the rats were anesthetized with isoflurane and euthanized (Kissin et al., 1983). Before euthanization, the groups treated with vehicle or 1-ABT underwent carotid angiography by exposing the suprarenal aorta and introducing an Echelon microcatheter (eV3 Neurovascular, Irvine, CA) with an Agility 10 microwire (Cordis, Miami, FL) into the abdominal aorta. Under fluoroscopic guidance (C-arm; Ziehm Imaging, Nurenberg, Germany), this microcatheter-wire system was navigated into the brachiocephalic artery and then into the left common carotid artery. Right and left carotid angiograms were obtained by injecting 0.6–0.8 ml of 50% diluted Omnipaque-300 (GE Healthcare, Princeton, NJ) by hand. All angiograms were taken in the anteroposterior (AP) plane. The microcatheter was then removed and the animal euthanized.

The Isite picture archiving and communication system (PACS) (Koninklijke Philips, Eindhoven, The Netherlands) was used to analyze the angiograms. The images used for analysis were those with the highest contrast opacification in the arterial phase. The percentage of carotid stenosis was calculated by using the North American Symptomatic Carotid Endarterectomy Trial (NASCET) formula (Ferguson et al., 1999) as follows: $1 - (a/c)$, where a is the residual luminal diameter at the stenosis and c is the luminal diameter at a visible, disease-free point above the stenosis. These measurements were performed in duplicate by the same individual who was blinded to the treatment groups.

Histology. At the end of the study, the left (injured) and right (uninjured) common carotid arteries were removed and flushed with normal saline to remove the blood. Each carotid was divided in two segments: one third was used for histomorphometric and immunohistochemical analysis and fixed in 10% buffered formalin; the remaining segment was used to measure the metabolism of AA. Twenty-four hours after fixation, the arterial segments were dehydrated, embedded in paraffin, and cut into 5-micron sections. Standard hematoxylin and eosin staining was performed on serial sections.

A computer imaging system equipped with Metamorph v6.37 (Molecular Devices, Sunnyvale, CA) was used to perform the histomorphometric analysis of the sectioned vessels. In brief, the luminal, internal elastic lamina, and external elastic lamina areas were manually measured. The intimal area was calculated as the internal elastic lamina area minus the luminal area; the medial area was calculated as the external elastic lamina area minus the internal elastic lamina area. The ratio of the intima to media area was then calculated. These measurements were performed by the same individual who was blinded to the treatment groups.

Immunohistochemistry. Paraffin-embedded tissue sections were deparaffinized in xylene and rehydrated through a gradient of ethanol solutions (100, 90, 80, and 70%) followed by extensive wash with Tris-buffered saline/Tween 20 (TBST; 0.08% Tween 20). Next, the antigens were retrieved by incubating sections with proteinase K solution (0.02 mg/ml in 10 mM Tris solution, pH 8.0) under humidified conditions at 37°C for 20 minutes. The sections were blocked in 1% bovine serum albumin (BSA) in TBST solution for 1 hour, followed by incubation with 1:200 dilution of the primary antibody to CYP4A (P4504A polyclonal goat antibody; Genetest) in 1% BSA/TBST solution at 4°C overnight.

After a rinse, the sections were incubated with secondary antibody (1:100 Alexa Fluor 488-conjugated rabbit, anti-goat Ab) at room temperature for 1 hour. The slides were then washed and incubated with a CY3-conjugated monoclonal antibody to smooth muscle actin (clone 1A4; Sigma-Aldrich) for 1 hour, washed, and counterstained with 4′,6-diamidino-2-phenylindole. Other sections were stained first with CYP4A primary antibody and the Alexa Fluor 488 conjugated secondary antibody and then were counterstained with 0.001% Evans blue to reduce green autofluorescence. The immunostained sections were examined using a fluorescent microscope interfaced with Metamorph 6.3 software.

Carotid Artery Cytochrome P450 Enzyme Assay. Fresh carotid arteries were collected and minced in 1 ml of cold physiologic salt solution. The vessel segments were incubated for 90 minutes at 37°C with a saturating concentration of AA (40 μM) in the presence of 1 mM NADPH and 2 μM indomethacin. The reactions were continuously shaken under an atmosphere of 100% O_2 to ensure adequate oxygenation of the incubation media. The reaction was stopped by acidification with formic acid to pH 3.5, and the vessels were homogenized until no tissue was visible. The homogenate was extracted twice with 3 ml of ethyl acetate after the addition of 2 ng of an internal standard d6-20-HETE. After centrifugation, the organic phase was collected and dried under nitrogen.

Assessment of the AA Metabolites (HETEs and EETs) Using Liquid Chromatography–Tandem Mass Spectrometry. Separation and quantification of arachidonic acid metabolites was accomplished using a Dionex Ultimate 3000 High-Performance Liquid Chromatography system equipped with an autosampler (Dionex, Banmockburn, IL) and a ABsciex 4000 Q trap tandem mass spectrometer with electrospray ionization (ABsciex, Foster City, CA). The samples were resuspended in acetonitrile and maintained at 4°C until dilution in 70% water just before injection into the high-performance liquid chromatography.

Separation of metabolites was achieved using a reverse phase column (Beta Basic C18, 150 X2.1 mm, 3 μm; Thermo Hypersil-Keystone, Bellefonte, PA), and the following mobile phase conditions were observed at a flow rate of 300 μl/min. Mobile phase A consisted of 90/8.5/1.4/0.1 (water/acetonitrile/acetic acid, v/v/v), and mobile phase B contained 85/15/0.1 (water/acetonitrile/acetic acid, v/v/v). The gradient was programmed at 67% A for 5 minutes, ramped to 54% B over 10 minutes, held at 54% B for 5 minutes, ramped to 94% B over

7 minutes, held at 94% B for 4.5 minutes, ramped to 33% in 0.3 minutes, and then held at 33% B for 4.2 minutes.

The mass spectrometer was operated in the negative ion mode and multiple reaction monitoring with the following instrument settings: ion spray voltage −4500 V, curtain gas 30, gas 1–50, temperature 600°C, gas 2–50, and unit resolution. The optimum collision energy, declustering potential, and exit potential for each transition were empirically determined using purchased standards. The transitions monitored for each AA metabolite were as follows: 337–201 (14,15-DiHETE); 337–167 (11,12-DiHETE); 337–127 (8,9-DiHETE); 319–231 (19-HETE); 319–245 (20-HETE); 319–261 (18-HETE); 337–145 (5,6-DiHETE); 319–233 (16-HETE); 319–175 (15-HETE); 319–149 (11-HETE); 319–179 (12-HETE); 319–155 (8-HETE); 319–203 (5-HETE); 319–175 (14,15-EET); 319–175 (11,12-EET); 319–257 (8,9-EET); 319–191 (5,6-EET); and 325–281/307 (d6-20-HETE) for the internal standard.

Quantitation of all of the AA metabolites was based on using d6-20-HETE as the internal standard for extraction efficiency. Standard curves were generated using a range of 0.02 to 20 ng/ml of each metabolite and 0.2 ng of d6-20-HETE.

Statistical Analysis. Data are presented as the mean value ± S.E.M. Statistical analysis was performed using SigmaStat v.3 software (Jandel Scientific, San Rafael, CA). The statistical significance of differences in mean values between groups were assessed by two-way analysis of variance (ANOVA) followed by Student-Newman-Keuls post hoc tests. $P < 0.05$ was considered statistically significant.

Results

Angiographic Analysis. The results of these experiments are presented in Fig. 1. Fourteen days after BI, the control rats developed an average carotid stenosis of 27.9 ± 2.6%. The degree of stenosis was reduced by 96% in rats treated with 1-ABT to 1.1 ± 0.7%. The effects of HET0016 on angiographic stenosis were not studied.

Histologic Analysis. The luminal surface was smooth, and the vascular wall was composed of only a few layers of cells with a large patent lumen in control carotid arteries (Fig. 2A). In contrast, there was marked intimal hyperplasia with reduced luminal area (0.14 ± 0.07 mm^2), increased intimal area (0.31 ± 0.02 mm^2), and increased intimal/medial ratios (2.02 ± 0.12) in BI vessels (Fig. 2B). Chronic treatment with 1-ABT or HET0016 markedly reduced neointima hyperplasia (Fig. 2, C and D) and resulted in a significant increase of the luminal area (0.29 ± 0.02 and 0.25 ± 0.02 mm^2, respectively) (Fig. 2E) and a decrease in the intimal area (0.10 ± 0.02 and 0.09 ± 0.02 mm^2, respectively) (Fig. 2F) and intimal/media ratios (0.79 ± 0.15 and 0.69 ± 0.21, respectively) (Fig. 2G) ($P < 0.001$).

HETE and EET Levels. Uninjured vessels produced DiHETEs; 20-, 15-, and 12-HETEs; and EETs when incubated with AA. The production of 20-HETE was statistically significantly elevated in BI vessels compared with the levels measured in uninjured vessels (Fig. 3A, light gray bar versus open bar: 0.96 ± 0.35 versus 0.50 ± 0.11 ng/mg tissue, respectively; $P < 0.01$). Chronic treatment with 1-ABT and HET0016 reduced the production of 20-HETE in BI vessels (Fig. 3A, dark gray bar and black bar, respectively; $P \leq 0.001$ versus injured control two-way ANOVA). The 14,15- and 11,12-diHETE levels were not statistically significant different

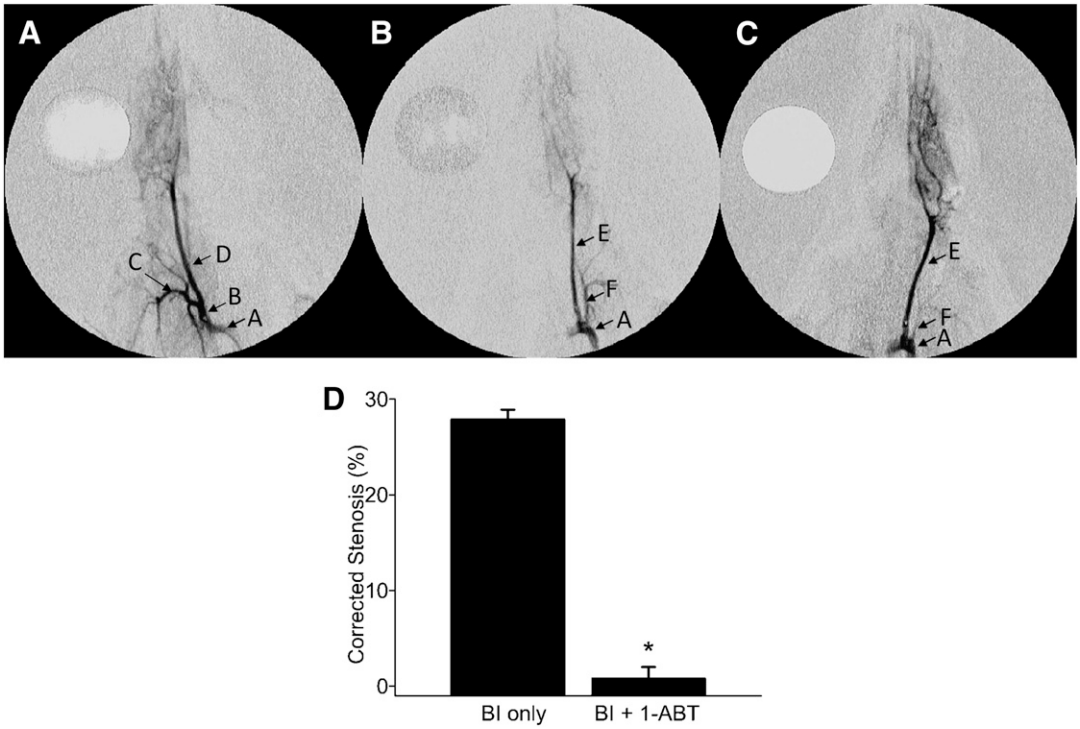

Fig. 1. Angiography analysis of carotid artery stenosis induced by balloon injury (BI). Anteroposterior angiograms of rat common carotid arteries 14 days after BI. (A) A representative image from an uninjured right control carotid artery. (B) Image from a BI left carotid artery. (C) Image from a BI carotid artery in a rat treated with 1-ABT. (D) Summary of the percentage change in angiographic stenosis in the BI left carotid arteries of control rats (BI only, $n = 10$) or rats chronically treated with 1-ABT (BI + 1-ABT, $n = 10$). The mean value ± S.E.M. is shown. *Statistically significant difference from the corresponding value in BI control rats. The mean value ± S.E.M. is shown. Arrows indicate the location of the aortic arch (A), brachiocephalic trunk (B), right subclavian artery (C), right common carotid artery (D), left common carotid artery (E), and left subclavian artery (F).

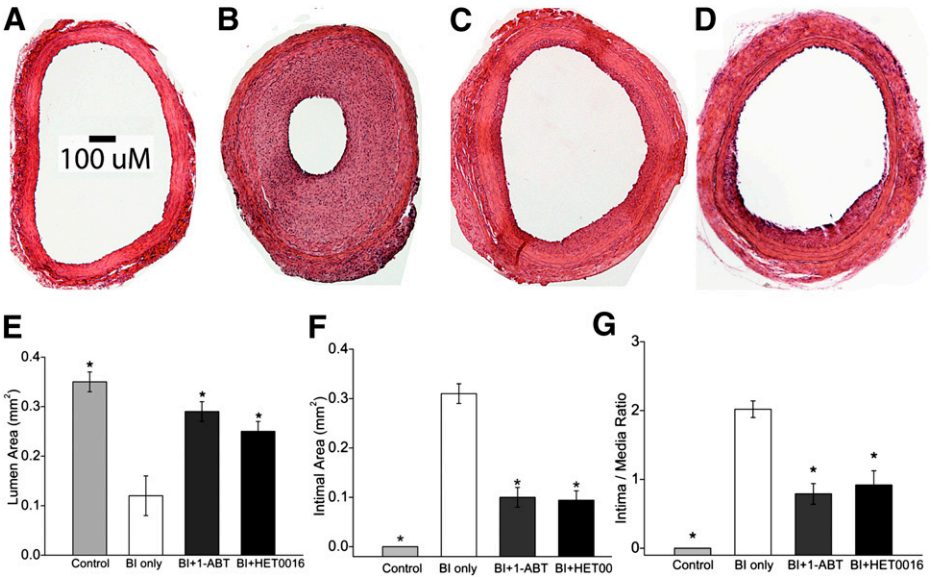

Fig. 2. Hematoxylin and eosin stain photomicrographs of rat common carotid artery sections 14 days after balloon injury (BI) at 100× magnification. The scale bar represents 100 μm. (A) Uninjured right carotid artery. (B) BI left carotid artery. (C) BI carotid artery of a 1-ABT-treated rat. (D) BI carotid artery of a HET-0016-treated rat. (E–G) Summary of the morphometric measurements of lumen area, intima area, and intima/media area ratio in left carotid arteries obtained from control rats (uninjured), rats that underwent BI alone, and rats that received BI and were treated with 1-ABT (BI + 1-ABT) or HET0016 (BI + HET0016). Data are presented as the mean values ± S.E.M. *Statistically significant difference from the corresponding value in BI control rats.

among the treatment groups in the control or BI vessels (Fig. 3, B and C), and the levels were not altered by administration of either ABT or HET0016.

Immunohistochemistry. CYP4A protein was largely expressed in the adventitia and in vascular smooth muscle cells of uninjured carotid arteries (Fig. 4A). The strong staining seen in the vascular wall is the well-known green autofluorescence of the elastic layers. There were marked increases in CYP4A expression in the intima of the carotid arteries subjected to BI, and CYP4A expression colocalized with staining for alpha-smooth muscle actin (Fig. 4B). The upregulation of the expression of CYP4A in infiltrating smooth muscle cells in the neointimal was even more apparent in the higher power image of a BI carotid artery (Fig. 5). Chronic treatment of the rats with 1-ABT or HET0016 significantly reduced neointima proliferation, intimal area, the upregulation of the expression of CYP4A in the neointima, and the number of smooth muscle actin-positive cells in the neointima (Fig. 4, C and D).

Discussion

Previous studies have indicated that 20-HETE can increase the migration and proliferation of VSMC in vitro but very little is known about the potential role of this compound in the pathogenesis of vascular injury in vivo (Stern et al., 1989; Lin et al., 1995; Bruijns et al., 1998; Muthalif et al., 1998; Uddin et al., 1998; Patricia et al., 1999; Reddy et al., 2002; Yaghini et al., 2005; Guo et al., 2007; Stec et al., 2007). Our study examined the contribution of 20-HETE into the development of neointimal hyperplasia after BI of the carotid artery of rats.

Our results indicate that 14 days after BI of the left carotid artery of rats, there is marked neointima hyperplasia associated with narrowing of the lumen of the vessel and an increase in the intima/media area ratio. The neointimal formation in the injured segment of the vessel is associated with a significant increase in the expression of CYP4A protein, especially in infiltrating VSMC in the neointima. Moreover, the production of 20-HETE was markedly elevated in BI segments of carotid arteries incubated with AA.

Additional experiments were performed to determine the role of the upregulation of CYP4A enzymes and the production of 20-HETE in neointimal formation after BI of the carotid artery. Chronic treatment of the rats with 1-ABT, which is an effective inhibitor of enzymes of the CYP4A family that produce 20-HETE, greatly reduced the infiltration of VSMC and IH after BI of the carotid arteries of Sprague Dawley rats. This was associated with a reduction in the formation of 20-HETE in the injured vessels back to the levels seen in control vessels. However, 1-ABT is not a specific inhibitor of the formation of 20-HETE, and it has been reported to also inhibit the activity of other P450 isoforms (CYP2B, 1A, 2C) that produce EETs in the liver, kidney, and lung (Balani et al., 2002; Xu et al., 2004; Miyata and Roman, 2005). Therefore, the experiments were repeated using HET0016, which is a chemically dissimilar and far more selective competitive inhibitor of the synthesis of 20-HETE (Miyata et al., 2001; Sato et al., 2001).

HET0016 has been reported to selectively inhibit the formation of 20-HETE at a concentration $<$35 nM. It has no effect on epoxygenase, cyclooxygenase, or lipoxygenase activities at concentrations up to 3 μM (Miyata et al., 2001; Sato et al., 2001); it also has minimal effects on the activity of other P450 isoforms involved in drug metabolism (Miyata et al., 2001; Sato et al., 2001; Xu et al., 2004; Miyata and Roman, 2005). Chronic treatment of the rats with HET0016 also inhibited neointimal hyperplasia and reduced the formation of 20-HETE in BI vessels.

Our finding that these two chemically and mechanistically different inhibitors of the synthesis of 20-HETE had similar effects to inhibit IH greatly diminishes the possibility that this is due to some shared off-target effect of these drugs and strongly supports the view that upregulation of the expression of CYP4A and the production of 20-HETE contribute to the proliferation and migration of vascular smooth muscle, neointimal formation, and vascular remodeling after endothelial injury.

Overall, the results of the present study are consistent with the previous report by Yaghini et al. (2005) indicating that administration of AA, angiotensin II, and 20-HETE enhanced

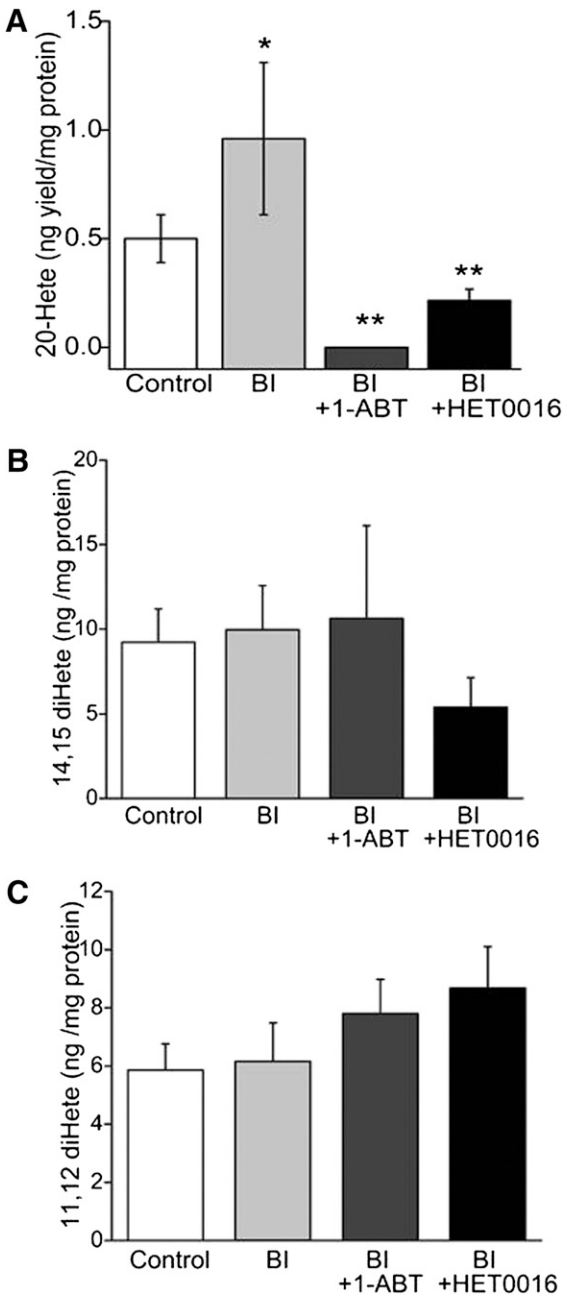

Fig. 3. 20-HETE (A), 14,15-dihydroxyeicosatetratenoic (14,15-diHETE) (B), and 11,12-dihydroxyeicosatetratenoic (11,12-diHETE) (C) levels were examined in uninjured right carotid arteries (control: open bars), injured left carotid arteries (light gray bar: BI), injured arteries with 1-ABT (BI + 1-ABT: dark gray bar), or HET0016 treatment (BI + HET0016: black bar). The HETE yield (ng) is calibrated with total protein (mg) used in the enzyme reactions. Data are presented as the mean ± S.E.M. *P = 0.003 compared with uninjured group. **$P < 0.001$ compared with injured group.

the expression of CYP4A1 and neointimal growth after BI of the carotid artery of rats and that administration of a CYP4A1 antisense oligonucleotide had no effect on neointima formation after BI alone. However, it attenuated the stimulatory effects of AA and angiotensin II but not exogenously administered 20-HETE on neointimal formation (Yaghini et al., 2005). Together, these data suggest that CYP4A metabolites of AA, most likely 20-HETE, mediate the stimulatory effects of angiotensin II on neointima formation after of the carotid arteries of rats.

The mechanism by which endothelial injury increases the formation of 20-HETE and contributes to IH remains to be determined. Chen et al. (2012) recently suggested that in normal vessels the expression of CYP4A is largely confined to the smooth muscle layers in the vessel wall and that locally produced 20-HETE contributes to the regulation of vascular tone. However, after endothelial injury through the loss of endothelial factors that tonically suppress the production of 20-HETE, the production of this compound increases. Supporting this view are the results of previous studies indicating that nitric oxide (NO), similar to carbon monoxide (CO), strongly binds to heme in CYP4A enzymes and inhibits the formation of 20-HETE in renal and hepatic microsomes and renal and cerebral arteries in vitro at concentrations <100 nM (Roman, 2002). After binding of NO, heme proteins are targeted for degradation and NO reduces the expression of the CYP4A protein. Thus, one can speculate that perhaps the normal endothelium through the formation of NO and CO limits the expression of CYP4A protein and the production of 20-HETE in VSMC in arteries.

After endothelial injury, the fall in the production of NO probably increases the local production of 20-HETE in the surrounding smooth muscle layers, and this contributes to the proliferation and migration of VSMC and neointimal hyperplasia. In this regard, 20-HETE has been previously reported to play a role in promoting the proliferation of a wide variety of cells in culture (Lin et al., 1995; Uddin et al., 1998; Muthalif et al., 2000), and P450 inhibitors attenuate the growth responses to serum, vasopressin, epidermal growth factor (EGF), and phorbol esters in cultured mesangial and epithelial cells and VEGF in human umbilical vein endothelial cells (HUVEC) (Lin et al., 1995; Roman, 2002; Sacerdoti et al., 2003; Zhao and Imig, 2003).

Several signal transduction pathways may be involved in the stimulation of cell growth after administration of 20-HETE to various cell types. Uddin et al. (1998) and Muthalif et al. (2000) reported that 20-HETE activates the mitogen-activated protein kinase (MAPK) pathway and stimulates the proliferation of cultured rat aortic VSMC. Muthalif et al. (1998, 2000) reported that activation of MAPK by norepinephrine and angiotensin II in VSMC is dependent on the formation of 20-HETE, which is generated after stimulation of cytosolic phospholipase A_2 by calcium/calmodulin-dependent protein kinase II. In addition, inhibition of the formation of 20-HETE prevented the effects of norepinephrine and angiotensin II to activate the MAPK system and promote the growth of aortic VSMC (Uddin et al., 1998). Stec et al. (2007) reported that 20-HETE induces migration of cultured VSMC. Chen et al. (2005) found that 20-HETE increases proliferation of human umbilical vein endothelial cells (HUVEC) in vitro and angiogenesis in the cornea of rats in vivo. Moreover, inhibitors of the formation of 20-HETE greatly attenuated the angiogenic response to VEGF, fibroblast growth factor (FGF), and epidermal growth factor (EGF) in the cornea (Chen et al., 2005).

Additional work by Muthalif et al. (2000) found that both norepinephrine- and 20-HETE-induced proliferation of VSMC involves translocation of the small G protein RAS to the membrane and activation of the MAPK pathway. Norepinephrine-induced activation of phospholipase D activity

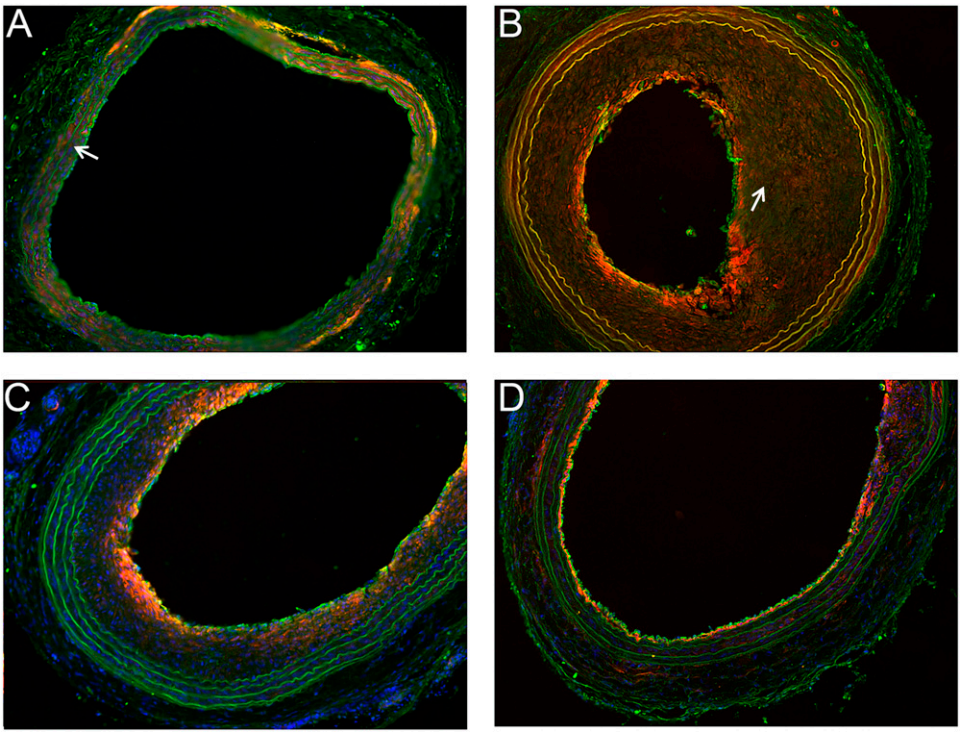

Fig. 4. CYP4A1 and vascular smooth muscle immunofluorescence staining. (A) Uninjured right carotid artery. (B) Balloon-injured (BI) left carotid artery of a rat treated with vehicle. (C) BI left carotid artery of a rat treated with 1-ABT. (D) BI carotid artery of a rat treated with HET-0016. Green: CYP4A1; red: VSMC-specific α-actin; blue: 4′,6-diamidino-2-phenylindole (DAPI)-stained nuclei. Note the lack of CYP4A1 (green) and α-actin (red) staining in the intima in normal uninjured arteries (arrows in panel A) and the marked increase in staining in the intima of BI arteries (arrows in panel B).

in rabbit VSMC is also coupled to the formation of 20-HETE and activation of MAPK pathway via a Ras-dependent mechanism. Thus, 20-HETE appears to couple receptors that activate phospholipases to activation of a MAPK signal transduction cascade in VSMC in a Ras-dependent manner (Muthalif et al., 1998, 2000).

As demonstrated in our study, by using currently available microcatheters and wires, we were able to evaluate in vivo the rat's carotid blood flow and lumen-wall interface. This angiographic technique provides several advantages over the evaluation of the lumen and vessel wall after it has been fixed. For instance, it allowed us to exclude arteries that were occluded by excessive balloon trauma, including dissection, rupture, and thrombosis (Orozco et al., 2011). More importantly, we noted a higher preservation of carotid artery diameter (96%) than one might expect from the suppression of IH alone in the rats treated with 1-ABT. This may be due in part to inhibition of the formation of 20-HETE and its vasoconstrictor properties and perhaps due to adaptive (outward) vascular remodeling seen in the vessels treated with inhibitors of the formation of 20-HETE. In this regard, our morphometric analysis indicated that luminal area increased by 107% in 1-ABT treated rats, compared with a 61–66% reduction in the neointima formation as measured by the intima/media ratio in rats treated with 1-ABT and HET0016, respectively. In this setting, inhibition of the formation of 20-HETE may have suppressed adventitial myofibroblasts, reducing not only the degree of IH but also that of constrictive vascular remodeling (Kundi et al., 2009).

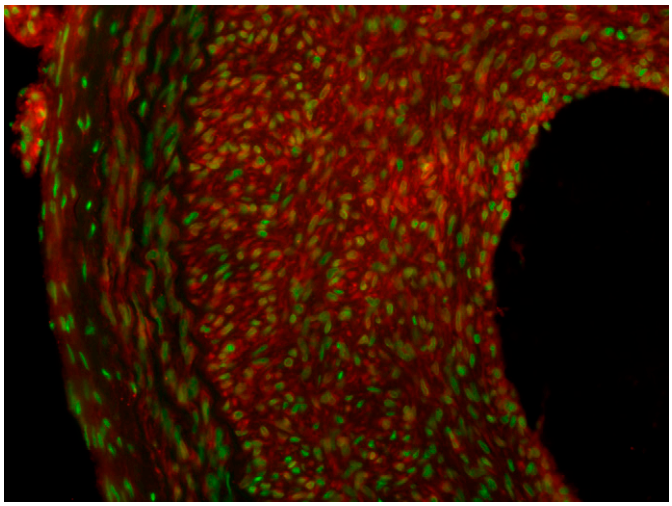

Fig. 5. High-power staining of CYP4A1 in balloon-injured (BI) rat carotid artery. The sections were stained with primary antibodies for CYP4A1 and Alexa Fluor 488 secondary antibody. The slide was counterstained with 0.01% trypan blue to quench the endogenous green fluorescence in the tissue. The image shows the positive green staining for the expression of CYP4A1 in infiltrating vascular smooth muscle cells in the neointima.

The mechanism of the vascular remodeling after systemic administration of 20-HETE inhibitors remains to be determined. One might suspect that blockade of the formation of 20-HETE might cause vascular remodeling by lowering arterial pressure. However, previous work by Hoagland et al. (2003) has indicated that chronic administration of ABT and HET0016 has little or no effect on blood pressure in Sprague Dawley rats fed a normal salt diet and produces salt-sensitive hypertension when rats are challenged with a high-salt diet. Thus, the changes in the vessel wall are not likely related to changes in systemic hemodynamics but rather are attributed to inhibition of the tonic stimulatory effects of 20-HETE on vascular growth.

Balloon injury of the rat common carotid artery is one of the most convenient and rapid models for IH, but it has been criticized for its failure to predict clinical efficacy of pharmacologic

interventions (Reidy et al., 1992; Bauters and Isner, 1997; Tulis, 2007). Thus, additional work will be needed to determine whether the present findings of a beneficial effect of 20-HETE inhibitors on IH in this rat model translate to humans.

The time course of IH after BI has been established. Initially, VSMC in the media proliferate and migrate to the intima. They continue to proliferate for 7–14 days to form an intimal thickening (Reidy et al., 1992; Bauters and Isner, 1997). In our study, the rats were sacrificed 14 days after BI at the peak of IH. BI promotes infiltration of leukocytes to the adventitia around the site of injury and increases production of cytokines and chemokines that contribute to neointimal growth (Hanke et al., 1990; Seki et al., 2000; Xing et al., 2004). AA metabolites such as 20-HETE are known to stimulate the inflammatory process initiated by mediators released from leukocytes and VSMC during injury. Polymorphonuclear leukocytes also synthesize 20-HETE, which could augment the inflammatory process, including increased adhesion of leukocytes to injured arteries and neointimal growth (Hill and Murphy, 1992; Okamoto et al., 2001; Xing et al., 2004).

Conclusion

Our present study demonstrates that the expression of CYP4A and the production of 20-HETE increase and contribute to neointimal growth in BI rat carotid arteries. In this setting, chronic administration of either 1-ABT or HET0016 suppressed 20-HETE production and inhibited neointimal formation and constrictive vascular remodeling. These findings suggest an important role of 20-HETE in the regulation of VSMC function, migration, and proliferation. Further characterization of these pathways along with the cell types that generate AA metabolites and their mechanisms of action could illuminate novel therapeutic targets for the treatment of restenosis, atherosclerosis, and other vascular diseases.

Acknowledgments

The authors thank Christine Purser for technical assistance with the analysis of the CYP metabolites of arachidonic acid.

Authorship Contributions

Participated in research design: Orozco, Perkins, Roman.

Conducted experiments: Orozco, Liu, Perkins, Johnson, Chen, Fan.

Contributed new reagents or analytic tools: Orozco, Liu, Chen, Fan, Baker, Roman.

Performed data analysis: Orozco, Liu, Perkins, Roman.

Wrote or contributed to the writing of the manuscript: Orozco, Liu, Roman.

References

Afergan E, Ben David M, Epstein H, Koroukhov N, Gilhar D, Rohekar K, Danenberg HD, and Golomb G (2010) Liposomal simvastatin attenuates neointimal hyperplasia in rats. *AAPS J* **12**:181–187.

Balani SK, Zhu T, Yang TJ, Liu Z, He B, and Lee FW (2002) Effective dosing regimen of 1-aminobenzotriazole for inhibition of antipyrine clearance in rats, dogs, and monkeys. *Drug Metab Dispos* **30**:1059–1062.

Bauters C and Isner JM (1997) The biology of restenosis. *Prog Cardiovasc Dis* **40**: 107–116.

Bruijns RH, van Kleef EM, Smits JF, De Mey JG, and Daemen MJ (1998) Effects of chemical sympathectomy on angiotensin II-induced neointimal growth in the balloon-injured rat carotid artery. *J Vasc Res* **35**:124–133.

Capdevila JH and Falck JR (2002) Biochemical and molecular properties of the cytochrome P450 arachidonic acid monooxygenases. *Prostaglandins Other Lipid Mediat* **68-69**:325–344.

Chen L, Ackerman R, and Guo AM (2012) 20-HETE in neovascularization. *Prostaglandins Other Lipid Mediat* **98**:63–68.

Chen P, Guo M, Wygle D, Edwards PA, Falck JR, Roman RJ, and Scicli AG (2005) Inhibitors of cytochrome P450 4A suppress angiogenic responses. *Am J Pathol* **166**: 615–624.

Davies MG and Hagen PO (1994) Pathobiology of intimal hyperplasia. *Br J Surg* **81**: 1254–1269.

Ferguson GG, Eliasziw M, Barr HW, Clagett GP, Barnes RW, Wallace MC, Taylor DW, Haynes RB, Finan JW, and Hachinski VC, et al. (1999) The North American Symptomatic Carotid Endarterectomy Trial: surgical results in 1415 patients. *Stroke* **30**:1751–1758.

Fujita H, Saito F, Sawada T, Kushiro T, Yagi H, and Kanmatsuse K (1999) Lipoxygenase inhibition decreases neointimal formation following vascular injury. *Atherosclerosis* **147**:69–75.

Guo AM, Arbab AS, Falck JR, Chen P, Edwards PA, Roman RJ, and Scicli AG (2007) Activation of vascular endothelial growth factor through reactive oxygen species mediates 20-hydroxyeicosatetraenoic acid-induced endothelial cell proliferation. *J Pharmacol Exp Ther* **321**:18–27.

Hanke H, Strohschneider T, Oberhoff M, Betz E, and Karsch KR (1990) Time course of smooth muscle cell proliferation in the intima and media of arteries following experimental angioplasty. *Circ Res* **67**:651–659.

Hill E and Murphy RC (1992) Quantitation of 20-hydroxy-5,8,11,14-eicosatetraenoic acid (20-HETE) produced by human polymorphonuclear leukocytes using electron capture ionization gas chromatography/mass spectrometry. *Biol Mass Spectrom* **21**:249–253.

Hoagland KM, Flasch AK, and Roman RJ (2003) Inhibitors of 20-HETE formation promote salt-sensitive hypertension in rats. *Hypertension* **42**:669–673.

Kissin I, Morgan PL, and Smith LR (1983) Comparison of isoflurane and halothane safety margins in rats. *Anesthesiology* **58**:556–561.

Kundi R, Hollenbeck ST, Yamanouchi D, Herman BC, Edlin R, Ryer EJ, Wang C, Tsai S, Liu B, and Kent KC (2009) Arterial gene transfer of the TGF-beta signalling protein Smad3 induces adaptive remodelling following angioplasty: a role for CTGF. *Cardiovasc Res* **84**:326–335.

Liang CJ, Ives HE, Yang CM, and Ma YH (2008) 20-HETE inhibits the proliferation of vascular smooth muscle cells via transforming growth factor-β. *J Lipid Res* **49**: 66–73.

Lin F, Rios A, Falck JR, Belosludtsev Y, and Schwartzman ML (1995) 20-Hydroxyeicosatetraenoic acid is formed in response to EGF and is a mitogen in rat proximal tubule. *Am J Physiol* **269**:F806–F816.

McGiff JC (1981) Prostaglandins, prostacyclin, and thromboxanes. *Annu Rev Pharmacol Toxicol* **21**:479–509.

Miyata N and Roman RJ (2005) Role of 20-hydroxyeicosatetraenoic acid (20-HETE) in vascular system. *J Smooth Muscle Res* **41**:175–193.

Miyata N, Taniguchi K, Seki T, Ishimoto T, Sato-Watanabe M, Yasuda Y, Doi M, Kametani S, Tomishima Y, and Ueki T, et al. (2001) HET0016, a potent and selective inhibitor of 20-HETE synthesizing enzyme. *Br J Pharmacol* **133**:325–329.

Muthalif MM, Benter IF, Karzoun N, Fatima S, Harper J, Uddin MR, and Malik KU (1998) 20-Hydroxyeicosatetraenoic acid mediates calcium/calmodulin-dependent protein kinase II-induced mitogen-activated protein kinase activation in vascular smooth muscle cells. *Proc Natl Acad Sci USA* **95**:12701–12706.

Muthalif MM, Benter IF, Khandekar Z, Gaber L, Estes A, Malik S, Parmentier JH, Manne V, and Malik KU (2000) Contribution of Ras GTPase/MAP kinase and cytochrome P450 metabolites to deoxycorticosterone-salt-induced hypertension. *Hypertension* **35**:457–463.

Okamoto E, Couse T, De Leon H, Vinten-Johansen J, Goodman RB, Scott NA, and Wilcox JN (2001) Perivascular inflammation after balloon angioplasty of porcine coronary arteries. *Circulation* **104**:2228–2235.

Orozco LD, Liu H, Chen BB, Fratkin JD, and Perkins E (2011) Angiographic evaluation of the rat carotid balloon injury model. *Exp Mol Pathol* **91**:590–595.

Patricia MK, Kim JA, Harper CM, Shih PT, Berliner JA, Natarajan R, Nadler JL, and Hedrick CC (1999) Lipoxygenase products increase monocyte adhesion to human aortic endothelial cells. *Arterioscler Thromb Vasc Biol* **19**:2615–2622.

Pietersma A, Kofflard M, de Wit LE, Stijnen T, Koster JF, Serruys PW, and Sluiter W (1995) Late lumen loss after coronary angioplasty is associated with the activation status of circulating phagocytes before treatment. *Circulation* **91**:1320–1325.

Reddy MA, Thimmalapura PR, Lanting L, Nadler JL, Fatima S, and Natarajan R (2002) The oxidized lipid and lipoxygenase product 12(S)-hydroxyeicosatetraenoic acid induces hypertrophy and fibronectin transcription in vascular smooth muscle cells via p38 MAPK and cAMP response element-binding protein activation. Mediation of angiotensin II effects. *J Biol Chem* **277**:9920–9928.

Reidy MA, Fingerle J, and Lindner V (1992) Factors controlling the development of arterial lesions after injury. *Circulation* **86**(Suppl)III43–III46.

Roman RJ (2002) P-450 metabolites of arachidonic acid in the control of cardiovascular function. *Physiol Rev* **82**:131–185.

Sacerdoti D, Gatta A, and McGiff JC (2003) Role of cytochrome P450-dependent arachidonic acid metabolites in liver physiology and pathophysiology. [Review] *Prostaglandins Other Lipid Mediat* **72**:51–71.

Samuelsson B (1983) Leukotrienes: mediators of immediate hypersensitivity reactions and inflammation. *Science* **220**:568–575.

Sato M, Ishii T, Kobayashi-Matsunaga Y, Amada H, Taniguchi K, Miyata N, and Kameo K (2001) Discovery of a N′-hydroxyphenylformamidine derivative HET0016 as a potent and selective 20-HETE synthase inhibitor. *Bioorg Med Chem Lett* **11**:2993–2995.

Seki Y, Kai H, Shibata R, Nagata T, Yasukawa H, Yoshimura A, and Imaizumi T (2000) Role of the JAK/STAT pathway in rat carotid artery remodeling after vascular injury. *Circ Res* **87**:12–18.

Stec DE, Gannon KP, Beaird JS, and Drummond HA (2007) 20-Hydroxyeicosatetraenoic acid (20-HETE) stimulates migration of vascular smooth muscle cells. *Cell Physiol Biochem* **19**:121–128.

Stern N, Golub M, Nozawa K, Berger M, Knoll E, Yanagawa N, Natarajan R, Nadler JL, and Tuck ML (1989) Selective inhibition of angiotensin II-mediated vasoconstriction by lipoxygenase blockade. *Am J Physiol* **257**:H434–H443.

Tulis DA (2007) Rat carotid artery balloon injury model. *Methods Mol Med* **139**:1–30.
Uddin MR, Muthalif MM, Karzoun NA, Benter IF, and Malik KU (1998) Cytochrome P-450 metabolites mediate norepinephrine-induced mitogenic signaling. *Hypertension* **31**:242–247.
Wu L, Zhu L, Shi WH, Yu B, and Cai D (2011) Zoledronate inhibits intimal hyperplasia in balloon-injured rat carotid artery. *Eur J Vasc Endovasc Surg* **41**:288–293.
Xing D, Miller A, Novak L, Rocha R, Chen YF, and Oparil S (2004) Estradiol and progestins differentially modulate leukocyte infiltration after vascular injury. *Circulation* **109**:234–241.
Xu F, Falck JR, Ortiz de Montellano PR, and Kroetz DL (2004) Catalytic activity and isoform-specific inhibition of rat cytochrome p450 4F enzymes. *J Pharmacol Exp Ther* **308**:887–895.
Yaghini FA, Zhang C, Parmentier JH, Estes AM, Jafari N, Schaefer SA, and Malik KU (2005) Contribution of arachidonic acid metabolites derived via cytochrome P4504A to angiotensin II-induced neointimal growth. *Hypertension* **45**:1182–1187.
Zhao X and Imig JD (2003) Kidney CYP450 enzymes: biological actions beyond drug metabolism. *Curr Drug Metab* **4**:73–84.

Address correspondence to: Dr. Ludwig D. Orozco, University of Mississippi Medical Center, Department of Neurosurgery, 2500 N. State Street, Jackson, MS 39216. E-mail: lorozco-castillo@umc.edu